Acta Cryst. (1986). A42, 560-569

Theory and Computation of Optical Rotatory Power in Inorganic Crystals

BY V. DEVARAJAN AND A. M. GLAZER

Clarendon Laboratory, University of Oxford, Parks Road, Oxford OX1 3PU, England

(*Received* 14 *May* 1986; *accepted* 30 *July* 1986)

Abstract

The classical polarizability theory of optical activity in crystals is elaborated and a method of calculating rotatory power from crystal structure data is described. By varying the polarizabilities of the atoms within reasonable limits, optical rotatory powers are computed for crystals of α-quartz, $AlPO_4$, cinnabar, $Bi_{12}SiO_{20}$, $Bi_{12}GeO_{20}$, α-$LiIO_3$, $NaClO_3$ and $NaBrO_3$. In general, the agreement between theory and experiment is excellent. As expected, considerable variability in polarizabilities is required in different structures in order to obtain satisfactory fits to the observed refractive indices and rotatory powers. The orientations of anisotropic polarizability ellipsoids derived in the course of the calculation are compared with those suggested earlier by Glazer & Stadnicka [*J. Appl. Cryst.* (1986), **19**, 108-122].

1. Introduction

There have been many attempts to correlate crystal structures and optical activity (OA), but in general these have met with little success. Even the association of the sign of optical rotation with the hand or chirality of the structure has, until recently, been contradictory, largely through numerous mistakes in determinations of absolute configuration. This problem has been described by Glazer & Stadnicka (1986), hereafter referred to as GS, who showed that it is, in fact, possible to link both structural and optical chiralities by using a simple visual approach based on the concept of anisotropic atomic polarizabilities.

In the present paper, we shall show that it is possible by theoretical calculation to make quantitative estimates of optical rotatory power in most of the inorganic crystals for which the absolute configuration is known. The theory described below involves the calculation of a microscopic polarizable ion model. The basic theory is not new, but various parts of it lie scattered throughout the literature, usually with different notations, often incomplete, and highly complex. It is very difficult, therefore, to find a complete theory of OA set out in a consistent manner. The problem of calculating optical properties such as OA was, to some extent, solved by the combined works of Ewald (1921), Born & Goeppert-Mayer (1933), and more recently by van Laar, Endeman & Bijvoet (1968). The mathematical techniques devised by these authors, and by others too, were used in a thesis by Reijnhart (1970)* to estimate optical rotation in several crystals, such as quartz, cinnabar *etc.* However, although some success in this was claimed, the absolute configurations of many of the crystals studied were either inaccurate or unavailable at the time. Nevertheless, we believe that Reijnhart's treatment was essentially correct, and in this paper we apply the technique to most of the crystals for which absolute configuration data are available. Reijnhart's treatment was never published outside his thesis. Because of this and the lack of coherence in much of the general literature on the subject of OA, and in order to correct some minor errors and misunderstandings, we set out below the full polarizability theory, which we have taken and adapted from many separate references. Using this theory, we compare computed values for optical rotatory powers with experimental measurements. We also use the theory to examine the anisotropic electronic polarizabilities of the atoms, which we represent by ellipsoids. These are compared with the 'guesses' made by GS, which were central to their visual explanation of the signs of optical rotation. It should be emphasized that the model and theory discussed below are purely classical and, therefore, are valid only for insulators, where the main contribution to OA comes from the electronic polarizabilities of individual atoms. For the same reason, it is also strictly applicable only in the long-wavelength regions above absorption (and circular dichroic) edges.

2. Theory

The theory of the calculation of optical activity in crystals is based on the fact that in most of the non-centrosymmetric crystals the dielectric constant shows a dispersion with wave vector. The dielectric displacement in an optically active, and non-absorbing, crystal is given as

$$\mathbf{D} = \varepsilon_0 \varepsilon_r \mathbf{E} + i\mathbf{G} \times \mathbf{E}, \qquad (1)$$

where ε_r is the relative dielectric permittivity tensor, $\mathbf{E}$ the electric field and $\mathbf{G}$ the so-called gyration vector

* Available upon request from Dr R. Reijnhart, Shell Research, Badhuisweg 3, 3031 CM Amsterdam, The Netherlands.

0108-7673/86/060560-10$01.50

parallel to the wave normal of the light. An *effective* dielectric tensor can then be defined by

$$\varepsilon'_{\text{eff}} = \varepsilon_0 \varepsilon_r + i[G], \tag{2}$$

where $[G]$ is an antisymmetric tensor. Thus the problem is one of calculating the dielectric permittivity, whose imaginary part contributes to the optical rotation.

The basic classical microscopic model for such a calculation was given earlier by Born & Huang (1954) and by Reijnhart (1970). In the following, we shall elaborate the details of the model and derive relations connecting the dielectric tensor, atomic positions and atomic polarizabilities in a crystal. This model assumes that the individual atoms behave like free atoms in the way they respond to an electromagnetic field. That is to say, the response of an atom s to an electromagnetic field E will be completely described by a point-dipole oscillator at its centre. The induced dipole-moment vector $\mathbf{p}_s$ is given by

$$\mathbf{p}_s = \alpha_s \mathbf{E}(\mathbf{r}_s), \tag{3}$$

where α_s is the polarizability tensor for atom s. $\mathbf{E}(\mathbf{r}_s)$ is the electric field at atom s, and originates from the dipole waves emanating from all the other atoms (point dipoles) in the crystal. Consequently, $\mathbf{E}(\mathbf{r}_s)$ is closely related to the crystal structure.

It is well known that this field consists of two parts (Born & Huang, 1954; Kittel, 1976), *i.e.*

$$\mathbf{E}(\mathbf{r}_s) = \mathbf{E}_{\text{ave}} + \mathbf{E}_{\text{loc}}, \tag{4}$$

where $\mathbf{E}_{\text{ave}}$ is the average field and $\mathbf{E}_{\text{loc}}$ is the local field. In isotropic cubic crystals $\mathbf{E}_{\text{loc}}$ corresponds to the Lorenz–Lorentz correction factor of $P/3\varepsilon_0$, where P is the average polarization. In a macroscopic, but finite, crystal the local field $\mathbf{E}_{\text{loc}}$ arises partly from the applied external field and partly from the environment (Kittel, 1976).

Ewald (1921) and Born & Huang (1954) considered the problem as follows. The crystal is thought to be made up from an infinite (*i.e.* very large) number of unit cells, and so the existence of an electromagnetic wave propagating inside the crystal in the direction of the wave vector $\mathbf{k}$ is described by adding a phase factor of $\exp(i\mathbf{k}\,.\,\mathbf{r}_s)$ to the dipoles ($\mathbf{p}_s$) at different atoms in the unit cell. If we restrict ourselves to the electronic part of the atomic polarizability (and thus to the visible region of the electromagnetic spectrum), the oscillating dipoles correspond to oscillating quasielastically bound valence electrons on the different atoms. The electromagnetic wave thus created will continue to exist only if the vibration of each dipole is just maintained by the field created by all the other dipoles acting together. Such an electromagnetic wave can be represented by a plane travelling wave having an angular frequency ω and a properly chosen wavelength λ inside the crystal. For this wave, we have the relations:

$$\begin{gathered} \omega = 2\pi c/\lambda_0 = 2\pi c/n\lambda, \\ k_0 = 2\pi/\lambda_0, \qquad |\mathbf{k}| = 2\pi/\lambda, \\ n = \lambda_0/\lambda = |\mathbf{k}|/k_0. \end{gathered} \tag{5}$$

λ_0, k_0 and c are the wavelength, wave vector and velocity of light *in vacuo*, $\mathbf{k}$ is the wave vector inside the crystal, and n is the refractive index. It is obvious that λ depends both on ω and on n. Using (3) and taking into account that the field at s is calculated by the sum of the dipole fields from all the other atoms in the crystal, we may write

$$\alpha_s^{-1} \mathbf{p}_s^l = \sum_{l's'}{}' \mathbf{E}_{s'}^{l'}(\mathbf{r}_s^l). \tag{6}$$

l denotes the cell index, and $\mathbf{E}_{s'}^{l'}(\mathbf{r}_s^l)$ is the electric field at the position of the atom s in cell l due to the dipole at (l', s'). The prime in the summation means that the field due to the dipole at (l, s) should be omitted. However, the field $\mathbf{E}_{s'}^{l'}(\mathbf{r}_s^l)$ is proportional to the dipole $\mathbf{p}_{s'}^{l'}$ and is a function of the vector between (l, s) and (l', s'). Thus, we can write

$$\mathbf{E}_{s'}^{l'}(\mathbf{r}_s^l) = a(\mathbf{r}_s^l - \mathbf{r}_{s'}^{l'})\mathbf{p}_{s'}^{l'}. \tag{7}$$

Hence (6) becomes

$$\alpha_s^{-1} \mathbf{p}_s^l = \sum_{l's'}{}' a(\mathbf{r}_s^l - \mathbf{r}_{s'}^{l'})\mathbf{p}_{s'}^{l'}. \tag{8}$$

For a plane wave in an infinite crystal,

$$\mathbf{p}_s^l = \mathbf{p}_s \exp(-i\omega t + i\mathbf{k}\,.\,\mathbf{r}_s^l), \tag{9}$$

and, substituting (9) into (8), we get

$$\alpha_s^{-1} \mathbf{p}_s = \sum_{s'}{}' \mathbf{p}_{s'} \left\{ \sum_{l'} a(\mathbf{r}_s^l - \mathbf{r}_{s'}^{l'}) \exp[-i\mathbf{k}\,.\,(\mathbf{r}_s^l - \mathbf{r}_{s'}^{l'})] \right\}, \tag{10}$$

where

$$\mathbf{r}_s^l = \mathbf{R}_l + \mathbf{r}_s,$$

$$\mathbf{R}_l = l_1\mathbf{a}_1 + l_2\mathbf{a}_2 + l_3\mathbf{a}_3,$$

and $\mathbf{a}_1$, $\mathbf{a}_2$ and $\mathbf{a}_3$ are the lattice vectors. Therefore, (10) becomes

$$\alpha_s^{-1} \mathbf{p}_s = \sum_{s'} \mathbf{p}_{s'} \left\{ \sum_{l'}{}' a(\mathbf{r}_s - \mathbf{r}_{s'} + \mathbf{R}_l - \mathbf{R}_{l'}) \times \exp[-i\mathbf{k}\,.\,(\mathbf{r}_s - \mathbf{r}_{s'} + \mathbf{R}_l - \mathbf{R}_{l'})] \right\}. \tag{11}$$

As the difference $(\mathbf{R}_l - \mathbf{R}_{l'})$ is involved in (11), the expression in braces is independent of the choice of unit-cell index. Thus, we may write

$$A(\mathbf{r}_s - \mathbf{r}_{s'}) = A_{ss'} = \sum_{l'}{}' a(\mathbf{r}_s^l - \mathbf{r}_{s'}^{l'}) \exp[-i\mathbf{k}\,.\,(\mathbf{r}_s^l - \mathbf{r}_{s'}^{l'})], \tag{12}$$

and then (10) becomes

$$\alpha_s^{-1} \mathbf{p}_s = \sum_{s'} A_{ss'} \mathbf{p}_{s'}, \tag{13}$$

and so, to solve (13), it is necessary to estimate $A_{ss'}$ and, consequently, $a(\mathbf{r}_s^l - \mathbf{r}_{s'}^{l'})$. This is done by the procedure given by Born & Goeppert-Mayer (1933) and by van Laar, Endeman & Bijvoet (1968), who calculated the electric field at (l, s) through the Hertz vector formalism (an oscillating dipole produces electromagnetic waves, which in turn excite other dipoles). According to this formalism, the *Hertz vector potential* at (l, s) due to all other dipoles is defined as

$$\mathbf{Z}_{s'}^{l'}(\mathbf{r}_s^l) = \sum_{l's'}{}' \mathbf{p}_{s'} \frac{\exp(-i\omega t + i\omega|\mathbf{r}_s^l - \mathbf{r}_{s'}^{l'}|/c)\exp(i\mathbf{k}.\mathbf{r}_{s'}^{l'})}{4\pi\varepsilon_0|\mathbf{r}_s^l - \mathbf{r}_{s'}^{l'}|}. \tag{14}$$

The factor $|\mathbf{r}_s^l - \mathbf{r}_{s'}^{l'}|/c$ is the time required for the electromagnetic wave originating from the oscillating dipole at (l, s) to reach (l', s'). This equation can now be recast as

$$\mathbf{Z}_{s'}^{l'}(\mathbf{r}_s^l) = \exp(-i\omega t)\sum_{s'}\mathbf{p}_{s'}\exp(i\mathbf{k}.\mathbf{r}_s^l) \times\left\{\sum_{l'}{}' \frac{\exp[ik_0|\mathbf{r}_s^l - \mathbf{r}_{s'}^{l'}| - i\mathbf{k}.(\mathbf{r}_s^l - \mathbf{r}_{s'}^{l'})]}{4\pi\varepsilon_0|\mathbf{r}_s^l - \mathbf{r}_{s'}^{l'}|}\right\}. \tag{15}$$

Again, the term in braces is independent of the choice of unit-cell index l' and has the periodicity of the lattice. Thus, this term can be decomposed into a Fourier series in reciprocal space given by

$$\sum_{l'}{}' \frac{\exp[ik_0|\mathbf{r}_s^l - \mathbf{r}_{s'}^{l'}| - i\mathbf{k}.(\mathbf{r}_s^l - \mathbf{r}_{s'}^{l'})]}{|\mathbf{r}_s^l - \mathbf{r}_{s'}^{l'}|} = \sum_h F_h^s \exp[i\mathbf{q}_h.(\mathbf{r}_s^l - \mathbf{r}_{s'}^{l'})], \tag{16}$$

where

$$F_h^s = \frac{1}{v}\int \frac{\exp(ik_0|\mathbf{r}_s^l - \mathbf{r}_{s'}^{l'}|)}{|\mathbf{r}_s^l - \mathbf{r}_{s'}^{l'}|} \times\exp[i(\mathbf{q}_h + \mathbf{k}).(\mathbf{r}_s^l - \mathbf{r}_{s'}^{l'})]\,dv. \tag{17}$$

v is the unit-cell volume and h is an integer triplet denoting the reciprocal-lattice vector

$$\mathbf{q}_h = h_1\mathbf{b}_1 + h_2\mathbf{b}_2 + h_3\mathbf{b}_3,$$

where $\mathbf{b}_1$, $\mathbf{b}_2$ and $\mathbf{b}_3$ are the reciprocal-cell axes. The integration extends over all space.

The sum in (16) is not absolutely convergent, and in order to achieve convergence, Ewald introduced the identity

$$\frac{\exp(ik_0|\mathbf{r}_s^l - \mathbf{r}_{s'}^{l'}|)}{|\mathbf{r}_s^l - \mathbf{r}_{s'}^{l'}|} = 2\pi^{-1/2}\int_0^\infty \exp(-|\mathbf{r}_s^l - \mathbf{r}_{s'}^{l'}|^2x^2 + k_0^2/4x^2)\,dx. \tag{18}$$

After applying his so-called Θ-function transformation, Ewald showed further that the sum in (16) may be split into two equivalent series, one in real space and one in reciprocal space. These are

$$F_1 = \sum_{l'} 2\pi^{-1/2}\int_0^\infty \exp[-|\mathbf{r}_s^l - \mathbf{r}_{s'}^{l'}|^2x^2 + k^2/4x^2 - i\mathbf{k}.(\mathbf{r}_s^l - \mathbf{r}_{s'}^{l'})]\,dx, \tag{19a}$$

$$F_2 = \sum_{h'}\frac{2\pi}{v}\int_0^\infty \frac{1}{x^3}\exp\{-[|\mathbf{q}_h + \mathbf{k}|^2 - k_0^2]/4x^2 + i\mathbf{q}_h.(\mathbf{r}_s - \mathbf{r}_{s'})\}\,dx. \tag{19b}$$

By interchange of the summation and integration, it is evident that the summation series in (19a) converges rapidly for large values of x, whereas the series in (19b) converges quickly for small values of x.

The sum in (16) can be considered to be made up of the two series in (19a) and (19b), with the condition that both should converge rapidly. We may divide the integral from 0 to ∞ into the sum of two integrals between W and ∞ for (19a) and between 0 and W for (19b), where W is a parameter chosen so as to ensure convergence. After integration, the sum $F_{lh} = F_1 + F_2$ becomes

$$F_{lh} = \sum_{l'} Wf(W|\mathbf{r}_s^l - \mathbf{r}_{s'}^{l'}|)\exp[-i\mathbf{k}.(\mathbf{r}_s^l - \mathbf{r}_{s'}^{l'})] + \frac{4\pi}{v}\sum_{h'}\frac{1}{[|\mathbf{q}_h + \mathbf{k}|^2 - k_0^2]} \times\exp\{-[|\mathbf{q}_h + \mathbf{k}|^2 - k_0^2]/4W^2 + i\mathbf{q}_h.(\mathbf{r}_s - \mathbf{r}_{s'})\}, \tag{20}$$

where

$$f(x) = (1/x) - (2/x\pi^{1/2})\int_0^x \exp(-\xi^2)\,d\xi. \tag{21}$$

Therefore, from (15), the Hertz vector may be written as

$$\mathbf{Z}_{s'}^{l'}(\mathbf{r}_s^l) = \frac{1}{4\pi\varepsilon_0}\sum_{s'}{}'\mathbf{p}_{s'}\exp(i\mathbf{k}.\mathbf{r}_s^l)\exp(-i\omega t)F_{lh}. \tag{22}$$

The electric field at $\mathbf{r}_s^l$ is given as

$$\mathbf{E}(\mathbf{r}_s^l)\text{grad div}\,\mathbf{Z}_{s'}^{l'}(\mathbf{r}_s^l) - \frac{1}{c^2}\frac{\partial^2\mathbf{Z}_{s'}^{l'}(\mathbf{r}_s^l)}{\partial t^2}, \tag{23}$$

and from (3)

$$\mathbf{E}(\mathbf{r}_s^l) = \alpha_s^{-1}\mathbf{p}_s^l. \tag{24}$$

Substituting (24) into (23) and using (22) and (9), we get

$$\alpha_s^{-1}\mathbf{p}_s = \frac{\exp(-i\mathbf{k}.\mathbf{r}_s^l)}{4\pi\varepsilon_0} \times\sum_{s'}\mathbf{p}_{s'}[F'_{lh} + k_0^2F_{lh}\exp(i\mathbf{k}.\mathbf{r}_s^l)], \tag{25}$$

where

$$F'_{lh} = \text{grad div}\,[F_{lh}\exp(i\mathbf{k}.\mathbf{r}_s^l)]. \tag{26}$$

Comparing (25) with (13), we find

$$A_{ss'}=\frac{1}{4\pi\varepsilon_0}\sum_{s'}{}' \mathbf{p}'_s[\exp(-i\mathbf{k}\,.\,\mathbf{r}^l_s)F'_{lh}+k_0^2F_{lh}]. \quad (27)$$

If we make use of the fact that k and k_0 are very small compared with the dimensions of the Brillouin zone for wavelengths in the visible region, we may expand the right-hand side of (27) in powers of $\mathbf{k}\,.\,\mathbf{r}$. Retaining only linear terms,

$$4\pi\varepsilon_0 A_{ss'}(\alpha\beta)=A^0_{ss'}(\alpha\beta)+i\sum_{\gamma}A^1_{ss'}(\alpha\beta,\gamma)\mathbf{k}_\gamma. \quad (28)$$

α, β and γ refer to the vector or tensor components in Cartesian coordinates. From Kellermann (1940), Born & Huang (1954) and van Laar *et al.* (1968), and with the relationships in (5), the following are derived:

$$\begin{aligned}A^0_{ss'}(\alpha\beta)&=(4\pi/v)[1/(n^2-1)](\delta_{\alpha\beta}-n^2u_{\alpha\beta})\\&\quad-\frac{4\pi}{vR^2}\sum_h{}'\mathbf{q}^\alpha_h\mathbf{q}^\beta_h G(|\mathbf{q}_h|^2/R^2)\\&\quad\times\exp[i\mathbf{q}_h\,.\,(\mathbf{r}_s-\mathbf{r}_{s'})]\\&\quad+R^3\sum_{l'}H_{\alpha\beta}(R\mathbf{r}^{l'}_{ss'})+\delta_{\alpha\beta}\delta_{ss'}4R^3/3\pi^{1/2},\end{aligned} \quad (29)$$

and

$$\begin{aligned}A^1_{ss'}(\alpha\beta,\gamma)&=-\frac{4\pi}{R^2v}\sum_h{}'(\mathbf{q}^\alpha_h\delta_{\beta\gamma}+\mathbf{q}^\beta_h\delta_{\alpha\gamma})G(|\mathbf{q}_h|^2/R^2)\\&\quad+(2/R^2)\mathbf{q}^\alpha_h\mathbf{q}^\beta_h\mathbf{q}^\gamma_h G'(|\mathbf{q}_h|^2/R^2)\\&\quad\times\exp[i\mathbf{q}_h\,.\,(\mathbf{r}_s-\mathbf{r}_{s'})]\\&\quad-2R^3\sum_{l'}H_{\alpha\beta}(R\mathbf{r}^{l'}_{ss'})\,.\,\mathbf{r}^{l'}_{ss'}.\end{aligned} \quad (30)$$

The term corresponding to $l'=0$ with $s=s'$ is ignored in the summation over l'; in the summation over h, the term $h=0$ should be omitted, and the various terms in (29) and (30) are

$$G(x)=\exp(-x)/x, \quad (31)$$

$$R=2W, \quad (32)$$

$$H_{\alpha\beta}(x)=\frac{x_\alpha x_\beta}{|x|^2}\Psi(|x|)-\delta_{\alpha\beta}\Phi(|x|), \quad (33a)$$

$$\Phi(x)=(1/x^3)\,\mathrm{erfc}\,(x)+2\exp(-x^2)/\pi^{1/2}, \quad (33b)$$

$$\Psi(x)=3\Phi(x)+4\pi^{-1/2}\exp(-x^2), \quad (33c)$$

$$\mathrm{erfc}\,(x)=1-2\pi^{-1/2}\textstyle\int_0^x\exp(-\xi^2)\,\mathrm{d}\xi, \quad (33d)$$

$$G'(x)=\mathrm{d}G(x)/\mathrm{d}\mathbf{k}_\gamma, \quad (34)$$

$$\mathbf{r}^{l'}_{ss'}=\mathbf{r}^{l'}+\mathbf{r}_{s'}-\mathbf{r}_s, \quad (35)$$

$$u_{\alpha\beta}=k_\alpha k_\beta/|\mathbf{k}|^2. \quad (36)$$

Now, (13) can be rewritten as

$$\sum_{s'}(\alpha_s^{-1}\delta_{ss'}-A_{ss'})\mathbf{p}_{s'}=0. \quad (37)$$

From (29) and (30), we may rewrite (28) as

$$A_{ss'}=\frac{1}{4\pi\varepsilon_0}Q_{ss'}+\frac{1}{v\varepsilon_0}\frac{I-n^2[U]}{n^2-1}, \quad (38)$$

where $[U]$ is a tensor with elements $u_{\alpha\beta}$. Substituting into (37) with the definition

$$\alpha_s^{-1}\delta_{ss'}-\frac{1}{4\pi\varepsilon_0}Q_{ss'}=B_{ss'}, \quad (39)$$

we get the relation

$$\sum_{s'}B_{ss'}\mathbf{p}_{s'}=\frac{1}{v\varepsilon_0}\frac{I-n^2[U]}{n^2-1}\sum_{s'}\mathbf{p}_{s'}. \quad (40)$$

Now, (40) can be reduced to a single vector equation in $\sum_{s'}\mathbf{p}_{s'}$. If there are p atoms per unit cell, we can form a $3p\times3p$ matrix whose elements are the $B_{ss'}$ (3×3) tensors. We may then define an inverse matrix whose corresponding 3×3 tensors we shall call $C_{ss'}$. Thus we get

$$\sum_s C_{s''s}B_{ss'}=I\delta_{s''s'}, \quad (41)$$

where I is the unit matrix. If one multiplies (40) by $C_{s''s}$, and sums over both s'' and s, followed by application of (41), it is seen that

$$\sum_{s'}\mathbf{p}_{s'}=\frac{1}{v\varepsilon_0}\sum_{s''s}C_{s''s}(I-n^2[U])(n^2-1)^{-1}\sum_{s'}\mathbf{p}_{s'}. \quad (42)$$

The macroscopic polarization is defined by

$$\mathbf{P}=(1/v)\sum_{s'}\mathbf{p}_{s'},$$

and so

$$\mathbf{P}=\frac{1}{v\varepsilon_0}\left[\sum_{s''s}C_{s''s}(I-n^2[U])(n^2-1)^{-1}\right]\mathbf{P}. \quad (43)$$

As $A_{ss'}$ is a complex tensor, the tensors $B_{ss'}$ and $C_{ss'}$ are also complex. By considering a plane electromagnetic wave travelling in a medium, Born & Huang (1954) showed that

$$\mathbf{P}=\frac{\varepsilon_r-1}{\varepsilon_0(n^2-1)}(I-n^2[U])\mathbf{P}. \quad (44)$$

Comparison with (43) gives

$$\varepsilon_r^{\alpha\beta}=\delta_{\alpha\beta}+(1/v)\sum_{s''s}C^{\alpha\beta}_{s''s}, \quad (45)$$

from which the relative dielectric permittivity may be calculated. From (1), the vector product $\mathbf{G}\times\mathbf{E}$ can always be represented by the product of an antisymmetric tensor $[G]$ and $\mathbf{E}$. The matrix elements

of $[G]$ are

$$G_{23} = -G_{32} = -\mathbf{G}_x,$$
$$G_{31} = -G_{13} = -\mathbf{G}_y, \qquad (46)$$
$$G_{12} = -G_{21} = -\mathbf{G}_z,$$

with diagonal terms equal to zero. It is this matrix that appears as $[G]$ in (2).

It is obvious that the imaginary part of $\sum C_{s''s}$ in (45) gives the $[G]$ tensor. Equation (28) shows that the imaginary part depends on the components of the wave vector which also defines the direction of propagation of the light. If **s** is the unit vector in the propagation direction, then

$$\mathbf{G} = G\mathbf{s} \qquad (47)$$

and G represents the magnitude of the gyration vector. Thus

$$\mathbf{s} \cdot \mathbf{G} = \mathbf{s}G\mathbf{s} = G\mathbf{s} \cdot \mathbf{s} = G. \qquad (48)$$

Consequently, if one knows the direction of propagation inside the crystal, the coefficient G can be calculated *via*

$$G = s_x G_{32} + s_y G_{13} + s_z G_{21} \qquad (49)$$

and then the optical rotatory power is defined as

$$\rho = -\pi G/\lambda_0 n. \qquad (50)$$

3. Details of calculation

From (29), (30), (39) and (41) we see that for the calculation of the tensor $C_{ss''}$ the atomic positions and the elements of the atomic polarizability tensors have to be supplied. Normally, for an atom in a general position in a crystal, there are six independent components (variables) in the polarizability tensor. Our approach was first to calculate the refractive indices ($n_x = \varepsilon_{xx}^{1/2}$ *etc.*) from (45). The atomic position coordinates were taken mainly from GS, and in all cases refer to the laevorotatory (−) enantiomorphs. In order to keep the numbers of unknown parameters to a minimum, we chose isotropic polarizability tensors (all diagonal elements the same and all off-diagonal elements set to zero), thus reducing the variables to one per atom.

A Fortran 77 program was written to carry out the calculations based on the above model. As the polarizabilities depend on the crystal structure and coordination, we varied them over a large range of values, but, nevertheless, kept them within acceptable limits, such as those given by Tessman, Kahn & Shockley (1953). We sometimes found it useful to plot the results in the form of contour diagrams in order to obtain an idea of the best combinations of polarizabilities to use. The atomic polarizabilities were then adjusted by trial and error until the calculated refractive indices were in reasonable agreement with the observed values, and then (50) gave the calculated values of the optical rotatory power. Further small adjustments to the isotropic polarizabilities were then made in some cases to get rotatory powers close to the observed values, but without compromising the calculated refractive indices. As a check, we were able with our program to obtain precisely the same numerical quantities as those obtained by Reijnhart when we used his polarizability values. In Table 1 the results of all the calculations are given. The polarizabilities are listed here as 'polarizability volumes' given by $\alpha' = \alpha/4\pi\varepsilon_0$. The rotatory powers quoted for the birefringent crystals refer to light propagating along the optic axis.

As a by-product of the method, we were able to obtain further information on the anisotropy of the atomic polarizabilities, which could be compared with those suggested earlier by GS. Although isotropic polarizability tensors were input to the program, the Ewald summation of the electric field renormalizes these tensors to reflect the effects of atom–atom interactions, thus in general making them anisotropic. An effective polarizability tensor α_s^{eff} for each atom, arising through the interaction of its dipole with those on other atoms (s'), was calculated using the expression

$$\alpha_s^{\text{eff}} = \sum_{s'} C_{ss'} \qquad (51)$$

which can be derived from (39) and (41). We took the symmetric part of the tensor α_s^{eff} to define a representational ellipsoid for the polarizability of the atom.

4. Discussion

Table 1 shows that, in general, an extremely good fit to the observed data has been achieved for many of the structures considered. In the following, unless specifically mentioned, the structural parameters used in each case were taken from the references given in GS.

In α-quartz, we calculated refractive indices and rotatory power using a large range of Si and O polarizabilities (but kept within acceptable limits). Fig. 1 shows a contour plot of computed values of ρ as a function of the Si and O polarizabilities. It can be seen that for most of the polarizabilities the sign of ρ remains negative with the magnitude increasing towards higher polarizabilities. Eventually, there is a sudden change in sign, as indicated in the top right corner of the figure. The contour for ρ corresponding to the experimentally observed value is marked by the heavy line. Contour plots for n_o and n_e over the same polarizability range showed that the contours corresponding to the experimental ordinary and extraordinary refractive indices were almost exactly superposable. This means that the theory gives the

Table 1. *Results of calculations for different crystals*

Crystal	λ(Å)	$\alpha' = \alpha/4\pi\varepsilon_0$ (Å^3)	n_o^{obs}	n_o^{cal}	n_e^{obs}	n_e^{cal}	ρ^{obs} (° mm^{-1})	ρ^{cal} (° mm^{-1})
α-SiO_2	5080	Si = 0·207 O = 1·213	1·548[f]	1·543	1·557[f]	1·551	−29·8[b]	−29·2
β-SiO_2	5170	Si = 0·185 O = 1·250	1·536[a]	1·534	1·544[a]	1·539	−34·2[c]	−30·7
α-HgS	6328	Hg = 0·000 S = 8·000	2·89[d]	2·74	3·24[d]	3·42	−320[e]	−312
α-$AlPO_4$	6328	Al = 0·05 P = 0·05 O = 1·37	1·521[f]	1·541	1·530[f]	1·545	−15[g]	−11·2
BSO	6500	Bi = 0·15 Si = 0·001 O = 3·54	2·550[h]	2·503			−20·5[i]	−19·5
BGO	6500	Bi = 0·025 Ge = 0·001 O = 3·725	2·540[f]	2·545			−19·5[i]	−33·5
α-$LiIO_3$	6328	Li = 0·03 I = 1·32 O = 1·55	1·88[j]	1·93	1·74[j]	1·60	−86·7[k]	−87·4
$NaClO_3$	6328	Na = 0·29 Cl = 0·01 O = 1·60	1·531[l]	1·526			−2·44[m]	−3·70
$NaBrO_3$	6328	Na = 0·29 Br = 0·10 O = 1·60	1·643[l]	1·498			−1·65[m]	+1·50

(a) Landolt-Börnstein (1962); (b) Szivessy & Münster (1934); (c) Lowry (1935); (d) Bond, Boyd & Carter (1967); (e) Ayrault, Lefin, Langlois, Toudic & Palmier (1972); (f) Landolt-Börnstein (1979); (g) Schwarzenbach (1966); (h) Lenzo, Spencer & Ballmann (1966); (i) Abrahams, Svensson & Tanguay (1979); (j) Nath & Haussühl (1969); (k) Stadnicka, Glazer & Moxon (1985); (l) Endeman (1965); (m) Abrahams, Glass & Nassau (1977).

correct birefringence of quartz. This contour is shown also in Fig. 1 by the thin line, and this cuts the thick line at just one place, where $\alpha'_{Si} = 0{\cdot}21$ and $\alpha'_O = 1{\cdot}21$ Å^3. Small adjustments in the polarizabilities gave the results shown in Table 1 for α-quartz.

α-quartz is one of the few crystalline materials for which optical rotation has been measured perpendicular to the optic axis, *i.e.* in a birefringent section. For laevorotatory quartz, Szivessy & Münster (1934) found it to be +13·3° mm^{-1} (note the change in sign). Using the same polarizabilities as in Table 1, we calculated it to be +19·5° mm^{-1}. This is in remarkably good agreement, not only in sign but also in magnitude, given that no new parameters were needed.

Fig. 2 shows plots of the structure on (0001) and along **a** with the computed anisotropic polarizabilities drawn as ellipsoids on each atom. This figure should be compared with the predictions made by GS [their Figs. 2(*b*) and 2(*c*)], where it can be seen that a very

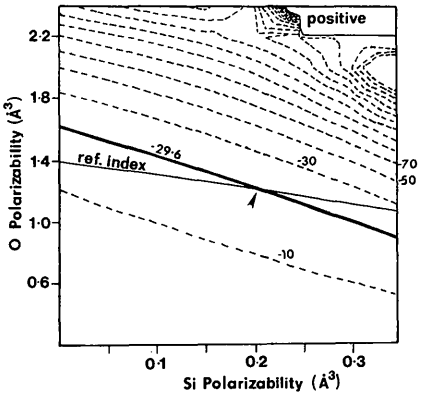

Fig. 1. Contour diagram showing how the calculated rotatory power varies with assumed polarizabilities for Si and O in α-quartz. The heavy full line indicates the contour corresponding to the observed rotation and the thin line indicates the path for the observed refractive index (ordinary and extraordinary curves are exactly superposed). The arrow marks their intersection.

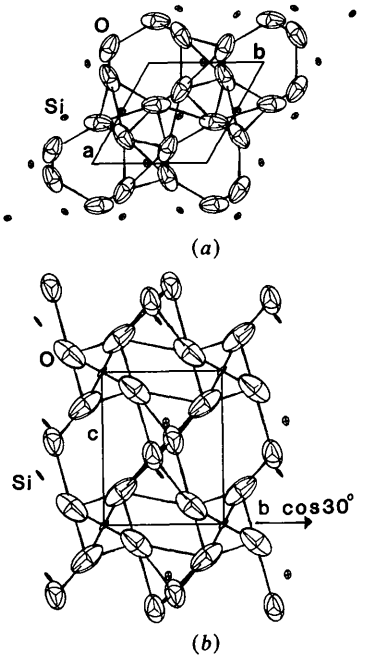

Fig. 2. Anisotropic polarizability ellipsoids for atoms in α-quartz, (*a*) projected on (0001) and (*b*) viewed along **a**. Compare with Figs. 2(*b*) and 2(*c*) in Glazer & Stadnicka (1986).

similar anisotropy was predicted by inspection. The success of this gives us further good reason to believe that our theoretical calculation is essentially correct and that it is more than a mere matter of fitting of data. The α-$AlPO_4$ or berlinite structure is in many respects a similar structure to that of quartz (see GS for a full discussion of the structure) and the calculations again give good results.

The β-quartz, or high-temperature structure, involves a straightening out of the oxygen tetrahedra, and according to GS this gives rise to a small increase in rotatory power. This increase has been measured by, for example, Lowry (1935), and our calculations again support this observation.

The results for α-HgS (the cinnabar structure) are particularly interesting and deserve close inspection. As pointed out by GS, there are two types of helices of sulfur atoms in the structure with opposite chiralities. Despite this, GS showed that the expected polarizability ellipsoids on the sulfur atoms were such that all the helices added together in their contribution to the overall rotatory power. Their explanation depended on the assumption that the polarizability of the Hg atom played an insignificant role in the problem. Fig. 3 shows the effect on the calculated rotatory power of varying the Hg and S isotropic polarizabilities over a large range of possible values. We see that a change in sign takes place in the middle of the diagram. The thick line corresponds to the observed rotation [a spread of observed values between $-303{\cdot}8$ and $335{\cdot}5°\ mm^{-1}$ is found in the work of Ayrault, Lefin, Langlois, Toudic & Palmier (1972), and so we have adopted $-320°\ mm^{-1}$ to be representative of HgS] and therefore this can be obtained over a range of Hg and S polarizabilities. However, for all these values we observed that $n_o^{cal} < n_o^{obs}$ and that $n_e^{cal} > n_e^{obs}$, and thus the calculated birefringence is not precisely the same as the observed value (this too was found by Reijnhart, who showed this to be due to inadequacies in the classical theory). We therefore calculated the average refractive index. This is shown by the thin line, representing the path of the correct average refractive index, and this intersects the thick line at a point where the polarizability of Hg is zero, in perfect agreement with the supposition made by GS. Moreover, the calculated anisotropic polarizabilities (Fig. 4) have precisely the same orientations as those predicted intuitively by GS [their Fig. 4(*b*)].

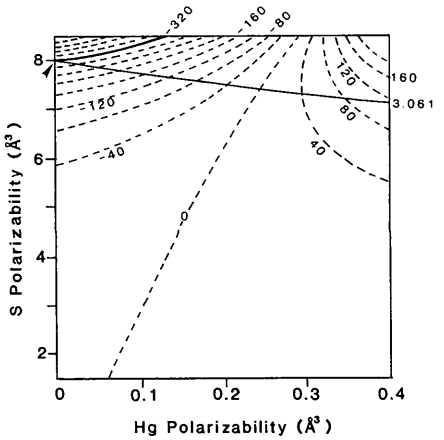

Fig. 3. Contour diagram showing how the calculated rotatory power varies with assumed polarizabilities for Hg and S. The heavy full line indicates the contour corresponding to the observed rotation and the thin line indicates the path for the observed average refractive index.

The structures of BSO and BGO ($Bi_{12}SiO_{20}$ and $Bi_{12}GeO_{20}$) are complicated, with a very large number of atoms in the unit cell. In this case, there are three isotropic polarizabilities to consider, and therefore more parameters to adjust. We assumed that the most important contribution to the OA must come from the oxygens, in line with the reasoning of GS, with silicon or germanium having a negligible polarizability, in order to reduce the calculation effectively to a two-parameter problem (in any case, there are very few Si/Ge atoms in the unit cell compared with the numbers of oxygens). With such a model we found that the best fit to the refractive index of BSO was 2·550 (observed) and 2·503 (calculated). While this is quite close, we wondered if it would be possible to improve on this. The calculated rotatory power was, in any case, very close to the observed value. In this structure, for which the space group is $I23(T^3)$, there are three distinct oxygen sites, O(1) at 24(*f*), O(2) at 8(*c*) and O(3) at 8(*c*) Wyckoff sites, and so a second model was tried in which we allowed the O(3), which are attached directly to the Si atoms, to adopt a slightly different polarizability from O(1) and O(2). This model thus gave an extra degree of freedom, and it was possible to get even closer to the observed refractive index without seriously affecting the rotatory power. In this computation the calculated refractive index was 2·552 and the rotatory power $-21{\cdot}7°\ mm^{-1}$ for polarizability volumes Bi = 0·06, Si = 0·001, O(1) = O(2) = 3·675 and O(3) = 3·575 Å^3. The calculated polarizability ellipsoids (Fig. 5) are again reminiscent of those predicted by GS [their

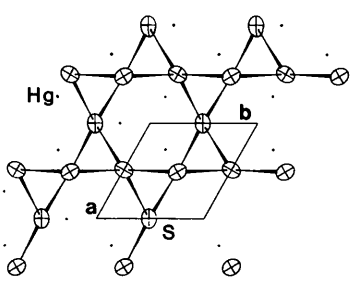

Fig. 4. Anisotropic polarizability ellipsoids for atoms in α-HgS projected on (0001). Compare with Fig. 4(*b*) in Glazer & Stadnicka (1986).

Fig. 6(*b*)], and, despite the complexity of this structure, our computed results show excellent agreement with observation.

We had some problems with BGO. Using the most recent structural data of Svensson, Abrahams & Bernstein (1979), the best fit to the refractive index gave a calculated rotatory power somewhat larger than that observed, although the sign came out right. We do not know why there is such a discrepancy, but it is worth noting that the structure determination indicates that the site occupancy of the Ge positions is only 0·87, and so there may be some imprecision in all the structural coordinates. The calculation of OA is very sensitive to small changes in atomic positions, particularly of the oxygens. Interestingly, when the older structural data of Abrahams, Jamieson & Bernstein (1967) were used with the same choice of polarizabilities, we obtained the refractive index as 2·553 and the rotatory power as $-23{\cdot}6°\ mm^{-1}$, a considerably better agreement with the observed rotation. We also note that the site occupancy of the Ge atom was 0·911 in this case.

Another interesting example is provided by α-$LiIO_3$. The absolute configuration was suggested by GS to have been incorrectly determined, and this was confirmed by Stadnicka, Glazer & Moxon (1985). The more rigorous theory presented here shows that, provided that iodine and oxygen polarizabilities are taken to be much larger than that of lithium (a most likely assumption), a good fit to the observed sign and magnitude of the rotatory power can be achieved, although the extraordinary refractive indices do not agree as well as might be expected. We feel, nevertheless, that our calculation is reasonably good: in this connection we note that, as in HgS, the average calculated refractive index is close to the observed value. The model also leads to polarizability ellipsoids (Fig. 6) that are in close agreement with those suggested by GS [their Fig. 8(*b*)].

In the final example, we come to the well known problem of the OA of $NaClO_3$ and $NaBrO_3$. It has been established (see GS) that if one considers the two structures in their equivalent chiral forms the optical rotations are observed to be opposite in sign. Several attempts have been made to calculate the rotatory power, by, for example, Hermann (1923) using Born's (1922) theory (he obtained the right order of magnitude but there was a numerical error in one of his equations). A full calculation, similar in essence to our own, was made by Beurskens-Kerssen, Kroon, Endeman, van Laar & Bijvoet (1963), who showed that the result depended sensitively on the exact positions chosen for the oxygens, although it should be noted that they did not include contributions from Na and Cl/Br. The size of the optical rotation is very close to zero for long wavelengths where the classical theory would apply, and so the sign is marginal. It would therefore be surprising if any classical theory, which is bound to be imperfect, could derive such small values with any confidence. Nevertheless, we made an attempt at the calculation. The initial results are given in Table 1.

Taking the Na polarizability to be that given by Tessman *et al.* (1953), the calculation for $NaClO_3$ gives a good fit to the observed rotation and refractive index. Fig. 7 shows the polarizability ellipsoids, which are in fair agreement with GS. However, for $NaBrO_3$, the laevo-structural data of Abrahams, Glass & Nassau (1977) led to a small positive optical rotation, with n^{cal} smaller than n^{obs}. All attempts at increasing n^{cal} made the computed rotatory power even larger and more positive. On the other hand, when we used structural parameters given by Hamilton (1938), we obtained $n^{cal} = 1{\cdot}495$ and $\rho^{cal} = -0{\cdot}15°\ mm^{-1}$ using the polarizability volumes Na = 0·29, Br = 0·01 and O = 1·65 Å^3. Although the refractive index has not improved, we see that it is just possible with the older structural data to obtain a change in sign of ρ.

Finally, it is worth considering the effect of changing the wavelength of the incident light in our calculation. To do this, it is not sufficient just to change the wavelength value used in the program, since this would not alter the computed refractive indices,

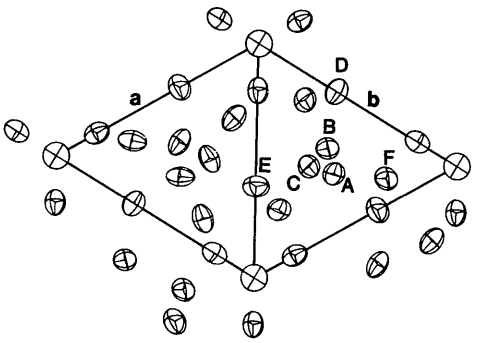

Fig. 5. Anisotropic polarizability ellipsoids for atoms in $Bi_{12}SiO_{20}$. The diagram shows one third of the unit cell projected on (111). The letters are those used by Glazer & Stadnicka (1986) in their Fig. 6(*b*).

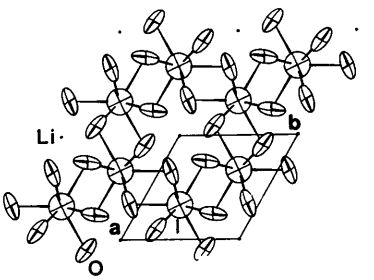

Fig. 6. Anisotropic polarizability ellipsoids for atoms in α-$LiIO_3$ projected on (0001). Compare with Fig. 8(*b*) in Glazer & Stadnicka (1986).

Table 2. *Calculations for α-quartz at different wavelengths*

λ (Å)	$\alpha' = \alpha/4\pi\varepsilon_0$ (Å^3)	n_o^{obs}	n_o^{cal}	n_e^{obs}	n_e^{cal}	ρ^{obs} (° mm^{-1})	ρ^{cal} (° mm^{-1})
1850	Si = 0·243 O = 1·421	1·658	1·695	1·690	1·709	−375·6	−412·3
3940	Si = 0·210 O = 1·232	1·558	1·556	1·568	1·564	−51·9	−51·6
4341	Si = 0·208 O = 1·223	1·554	1·550	1·563	1·557	−41·9	−41·3
4861	Si = 0·207 O = 1·216	1·550	1·545	1·559	1·553	−32·8	−32·3
5080	Si = 0·207 O = 1·213	1·548	1·543	1·557	1·551	−29·8	−29·2
5461	Si = 0·206 O = 1·209	1·546	1·541	1·555	1·548	−25·5	−25·0
5893	Si = 0·206 O = 1·206	1·544	1·539	1·553	1·546	−21·7	−21·3
6563	Si = 0·205 O = 1·201	1·542	1·536	1·551	1·543	−17·3	−16·9

The values of observed rotatory power were obtained for each wavelength using the formula given for quartz by Lowry (1935), p. 258.

which depend only on the choice of polarizabilities. It is necessary therefore to change the values of the polarizabilities too. Taking as an example α-quartz, for which the most extensive data are available, we started with the polarizabilities in Table 1 and used the Clausius–Mosotti relationship,

$$(n^2-1)/(n^2+2) = k\alpha,$$

to find the scale factor k (averaged for ordinary and extraordinary refractive indices). This was then reinserted into the Clausius–Mosotti formula together with the known refractive indices at other wavelengths and then used to calculate the relevant polarizabilities. The same scale factor was applied to both Si and O. In this way, we determined a set of polarizabilities as a function of wavelength which were scaled to the observed refractive indices, but which originated only from the polarizabilities already found in Table 1. Table 2 gives the results of the computations and Fig. 8 shows the observed and calculated optical rotations plotted as a function of wavelength. The agreement between them is very satisfying.

5. Concluding remarks

Optical activity arises from a delicate balance between the velocities of left- and right-circular components of visible light on passing through a chiral crystal. In spite of this very small difference in velocities, we have shown that by using classical theories originally developed many years ago by Born and others, it is usually possible to compute refractive indices and hence rotatory powers from inorganic crystal structure parameters and isotropic atomic polarizabilities. The results generally show good agreement with observation. Table 1 shows that in order to obtain satisfactory fits to the observed refractive indices and, at the same time, the observed rotatory powers, the polarizability values have to vary from compound to compound. Thus, as has been pointed out many times before by others, we find that there is a large variation of values for the oxygen atoms in crystals. One important by-product of this type of calculation is that we can obtain an estimate of the anisotropic polarizabilities of atoms within a particular structure. Calculations such as these, and intuitive theories such as the one given by GS, give a great deal of insight

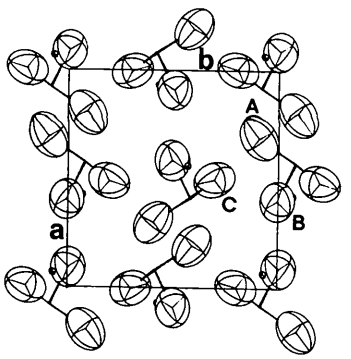

Fig. 7. Anisotropic polarizability ellipsoids for atoms in $NaClO_3$ projected on (001). The letters are those used by Glazer & Stadnicka (1986) in their Fig. 7(*a*).

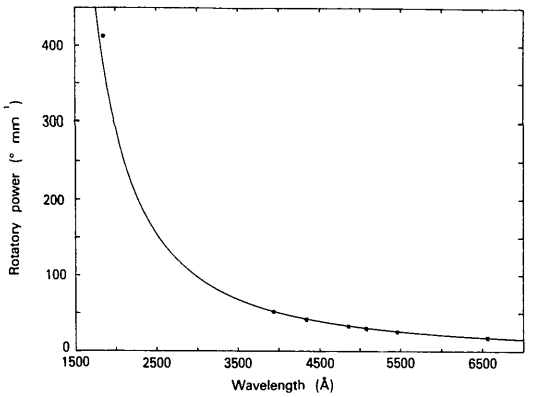

Fig. 8. Plot of computed (*) and observed (continuous curve) rotatory powers for α-quartz as a function of wavelength.

into the origin of the phenomenon of OA. In particular, they allow one to determine the relative roles of the constituent atoms in the structure and thus to suggest how the optical rotation could be modified in a particular crystal.

We thank Professor F. Tuinstra for drawing our attention to the thesis by Reijnhart (1970). We are grateful for a research grant from Jesus College, Oxford, and also to the Science and Engineering Research Council and Plessey Ltd for a JOERS grant, which made this work possible. We also wish to express our gratitude to the referees for their invaluable comments on this work.

References

ABRAHAMS, S. C., GLASS, A. M. & NASSAU, K. (1977). *Solid State Commun.* **29**, 515-516.

ABRAHAMS, S. C., JAMIESON, P. B. & BERNSTEIN, J. L. (1967). *J. Chem. Phys.* **47**, 4034-4041.

ABRAHAMS, S. C., SVENSSON, C. & TANGUAY, A. R. (1979). *Solid State Commun.* **30**, 293-295.

AYRAULT, B., LEFIN, F., LANGLOIS, H., TOUDIC, Y. & PALMIER, J. F. (1972). *Optics Commun.* **5**, 239-243.

BEURSKENS-KERSSEN, G., KROON, J., ENDEMAN, H. J., VAN LAAR, J. & BIJVOET, J. M. (1963). *Crystallography and Crystal Perfection*, edited by G. RAMACHANDRAN, pp. 225-236. London: Academic Press.

BOND, W. L., BOYD, G. D. & CARTER, H. L. (1967). *J. Appl. Phys.* **38**, 4090-4091.

BORN, M. (1922). *Z. Phys.* **8**, 390-417.

BORN, M. & GOEPPERT-MAYER, M. (1933). *Dynamische Gittertheorie der Kristalle.* In *Handbuch der Physik*, Vol. 24, pp. 623-794.

BORN, M. & HUANG, K. (1954). *Dynamical Theory of Crystal Lattices.* Oxford: Clarendon Press.

ENDEMAN, H. J. (1965). *Berekening van de Optische Activiteit van Natriumchloraat en bromaatkristallen en van α-Kwarts.* Dissertation, Utrecht.

EWALD, P. P. (1921). *Ann. Phys. (Leipzig)*, **64**, 253-287.

GLAZER, A. M. & STADNICKA, K. (1986). *J. Appl. Cryst.* **19**, 108-122.

HAMILTON, J. E. (1938). *Z. Kristallogr.* **100**, 104-110.

HERMANN, C. (1923). *Z. Phys.* **16**, 103-134.

KELLERMANN, E. W. (1940). *Philos. Trans. R. Soc. London Ser. A*, **238**, 513-548.

KITTEL, C. (1976). *Introduction to Solid State Physics.* New York: John Wiley.

LAAR, J. VAN, ENDEMAN, H. J. & BIJVOET, J. M. (1968). *Acta Cryst.* A**24**, 52-56.

LANDOLT-BÖRNSTEIN (1962). *Zahlenwerte und Funktionen*, Band II. Berlin: Springer.

LANDOLT-BÖRNSTEIN (1979). *New Series*, Vol. 11. Berlin: Springer.

LENZO, P. V., SPENCER, E. G. & BALLMANN, A. A. (1966). *Appl. Opt.* **5**, 1688-1689.

LOWRY, T. M. (1935). *Optical Rotatory Power.* London: Longmans.

NATH, G. & HAUSSÜHL, S. (1969). *Appl. Phys. Lett.* **14**, 154-156.

REIJNHART, R. (1970). *Classical Calculations Concerning the Double Refraction, Optical Rotation and Absolute Configuration of* Te, Se, *Cinnabar* (HgS), *α- and β-Quartz, β-Cristobalite,* $NaNO_2$, $NaClO_3$ *and* $NaBrO_3$. Dissertation, Delft.

SCHWARZENBACH, D. (1966). *Z. Kristallogr.* **123**, 161-185.

STADNICKA, K., GLAZER, A. M. & MOXON, J. R. (1985). *J. Appl. Cryst.* **18**, 237-240.

SVENSSON, C., ABRAHAMS, S. C. & BERNSTEIN, J. L. (1979). *Acta Cryst.* B**35**, 2687-2690.

SZIVESSY, G. & MÜNSTER, C. (1934). *Ann. Phys. (Leipzig)*, **20**, 703-726.

TESSMAN, J., KAHN, A. & SHOCKLEY, W. (1953). *Phys. Rev.* **92**, 890-895.

Acta Cryst. (1986). A**42**, 569-577

Convergent-Beam Reflection High-Energy Electron Diffraction (RHEED) Observations from an Si(111) Surface

BY G. LEHMPFUHL

Fritz-Haber-Institut der Max-Planck-Gesellschaft, Faradayweg 4-6, *D*-1000 *Berlin* 33, *Federal Republic of Germany*

AND W. C. T. DOWELL

CSIRO Division of Chemical Physics, Clayton, Victoria, Australia

(*Received* 26 *March* 1986; *accepted* 18 *July* 1986)

Abstract

Conditions for the intensity enhancement of a Bragg reflection are investigated through convergent-beam (CB) reflection electron diffraction experiments. This intensity enhancement is of great interest for reflection electron microscopy of surfaces. Comparison of CB reflection diffraction patterns with CB transmission diffraction patterns shows a very similar enhancement which can be explained by Bloch waves. The observed surface diffraction parabolae are closely related to Kikuchi envelopes. The intensity enhancement can be interpreted as a channelling phenomenon.

0108-7673/86/060569-09$01.50